SUPERSONIC WINGS WITH SIGNIFICANT LEADING-EDGE THRUST AT CRUISE

A. Warner Robins, Harry W. Carlson, and Robert J. Mack
Langley Research Center

SUMMARY

Experimental/theoretical correlations are presented which show that significant levels of leading-edge thrust are possible at supersonic speeds for certain planforms which match the theoretical thrust-distribution potential with the supporting airfoil geometry. The new analytical process employed provides not only the level of leading-edge thrust attainable but also the spanwise distribution of both it and/or that component of full theoretical thrust which acts as vortex lift. Significantly improved aerodynamic performance in the moderate supersonic speed regime is indicated.

INTRODUCTION

Aerodynamicists have long known of the importance of leading-edge thrust to the performance of subsonic aircraft. These forces, which arise from the very low pressures induced by the high velocities of the flow around the leading edge from a stagnation point beneath the wing, largely counteract the drag from the remainder of the airfoil in high-aspect-ratio wings at low speeds. Very high aerodynamic efficiency for such wings is the result. The efforts to extend these benefits to the higher speeds have led to the swept wings commonly seen in present-day, long-range aircraft. Indeed, according to theory, should wing leading edges be swept sufficiently behind the Mach angle, there is potential for leading-edge thrust at supersonic speeds. Until very recently (refs. 1 and 2), however, the potential for leading-edge thrust at cruise in configurations suitable for extended supersonic cruising was generally thought to be negligible. It is the purpose of this paper to show that such is not the case, that certain planforms favor supersonic leading-edge thrust, and that with a new method for predicting the degree to which it exists as well as predicting its spanwise distribution, there exists some rationale for the exploitation thereof.

SYMBOLS

b wing span

c wing chord length

$\bar{c}$ mean aerodynamic chord

C_D drag coefficient

C_L	lift coefficient
$C_{L,opt}$	lift coefficient at maximum lift-drag ratio
C_m	pitching moment coefficient
C_A	axial or chord force coefficient
C_p	pressure coefficient
C_t	local thrust coefficient
C_T	total thrust coefficient, $2\int_0^{b/2} C_t d_y$
L/D	lift-to-drag ratio, C_L/C_D
M	free-stream Mach number
RN	free-stream Reynolds number
sfc	specific fuel consumption
t	maximum thickness of local wing chord
x	longitudinal distance to local wing leading edge
y	spanwise distance from reference axis
α	angle of attack, deg
β	$= \sqrt{M^2 - 1}$
Λ	leading-edge sweep angle

Subscript:

$\bar{c}$	referenced to mean aerodynamic chord
l	denotes limiting condition
n	quantities pertaining to a wing section normal to leading edge
max	denotes maximum value

DISCUSSION

Experimental/Theoretical Considerations

An experimental/theoretical comparison of the drag polars of three slender supersonic-cruise configurations is shown in figure 1. The two on the left which were tested at Mach number 2.7 were the last competing pair in the national SST program. The configuration on the right, which is an NASA concept (ref. 3) of essentially the same vintage, was tested at Mach number 2.6. All were tested in the NASA Langley Unitary Plan wind tunnel at a Reynolds number, based on mean aerodynamic chord, of approximately 5 million.

All three configurations have subsonic leading edges over much of the wing span (that is; local leading edge swept behind the Mach line), and the leftmost concept has blunt airfoil sections; conditions conducive to leading-edge thrust. The generally good agreement between experiment and calculation (refs. 4, 5, 6) in which measured drag generally exceeds theory by small amounts, if any, would suggest some validity in the generally accepted assumption of no leading-edge thrust in the calculation methods. These data seem characteristic of supersonic drag polars at design speed, generally. Thus, supersonic design and evaluation methods have generally (and, perphaps, conveniently) neglected leading-edge thrust.

Some insight into the lack of evidence of supersonic leading-edge thrust may be gained from figure 2. Here theoretical maximum thrust and bluntness or thickness comparisons are shown (with thickness somewhat exaggerated for clarity) for two planforms having predominantly subsonic leading edges. In the case of the more conventional straight-leading-edge wing where there is potential for thrust, there is little thickness or bluntness for it to act upon. The complex-leading-edge wing, however, with its higher inboard sweep (reaching almost 80 degrees) and fuller inboard thickness shows a significant thrust potential where the geometry favors its attainment. Put another way, there is upwash where there is thickness. Experimental/theoretical comparisons of static longitudinal aerodynamic characteristics of a wing model having the planform of this complex wing will subsequently be shown. The model (ref. 1) had a design Mach number of 1.8, a design lift coefficient of 0.07, and NACA 65A004 airfoil sections and was essentially a wing alone, having a small balance housing mounted essentially symmetrically about the camber plane and faired smoothly into the forward surfaces of the wing. As shown in figure 3, tests were conducted at the design Mach number of 1.8 and at a Reynolds number, based on mean aerodynamic chord, of about 2 million. Compare first the experimental data with the no-leading-edge-thrust linear theory (refs. 7, 8, 9) without pressure-coefficient limiting or consideration of vortex lift (refs. 10 and 11). The experimental nonlinearities in the lift curve and in the pitching moment, in particular, are not represented by theory, nor is there adequate representation of lift-drag ratio at optimum lift (that is; lift coefficient for maximum lift-drag ratio). Arbitrarily limiting the linear-theory pressure coefficients (which might otherwise be below vacuum) to 3/4 vacuum results in the dashed curves. Breaks are now seen in the theory curves which would seem to result from significant and progressive lift losses from the tip region inboard, indicated by the severity of the pitching moment nonlinearity, Thus it would seem that

theory without pressure constraint calls for potential-flow pressures which physically cannot be achieved. Some other flow mechanism must therefore have existed. Assuming that, when potential flow cannot be fully maintained, the Polhamus vortex-lift analogy (ref. 10) applies, normal force increments representing the effects of separated vorticity were then applied to the limited linear theory values. These lift increments were obtained by a new method (ref. 12) which provides the necessary theoretical full leading-edge-thrust values for the arbitrary planform. The resulting theoretical values are seen (fig. 3) as the dot-dash curve. These curves of limited linear theory with vortex lift, all parameters considered, are certainly an improvement, but there remains a large discrepancy in maximum lift-drag ratio.

On the assumption that, prior to manifesting itself as vortex lift, some leading-edge thrust might, indeed, have occurred, the final curve showing the pressure-coefficient-limited linear theory without vortex lift but with full theoretical thrust is presented. Agreement at maximum lift-drag ratio is much improved. There remains, however, a problem beyond predicting leading-edge thrust or vortex lift at supersonic speeds, and that is the analytical representation of the transition from the thrusting mode to the vortex-lift mode.

New Analytical Method

A new method (ref. 13) for estimation of attainable thrust has been developed and the key features thereof are presented in figure 4. The method applies simple sweep theory to wings of arbitrary planform, permitting two-dimensional analysis. A comprehensive survey of two-dimensional data is correlated to provide limiting-pressure restraints as a function of these normal Mach and Reynolds numbers. Correlation equations derived from theoretical two-dimensional data then provide thrust-coefficient limitation as a function of theoretical thrust, limiting pressure, and airfoil section parameters. With these relationships programmed as a subroutine in existing lifting-surface programs, spanwise distribution of attainable thrust is directly available for use in lift and drag estimation. These lift and drag relationships are compatible with the Polhamus leading-edge-suction analogy for fully detached leading-edge flow when the analogy is taken to be the limiting case of a gradual rotation of the full suction vector as leading-edge thrust is lost. Thus the method does provide a rational analytical means for making the transition from the thrust mode to that of vortex lift.

In figure 5, experimental axial-force coefficient--a parameter sensitive to leading-edge thrust--is compared over the lift range to theoretical values for full leading-ledge thrust and for no leading-edge thrust, as well as for the attainable-thrust values from the new method. Not only is a significant amount of experimental leading-edge thrust indicated, but a reasonably good representation of experiment by the new attainable-thrust method is obtained in the positive-lift range up to lift coefficients of 0.3 or so.

Returning via figure 6 to the lift-drag ratio comparisons between theory and experiment, the attainable curve is seen to agree with the full-thrust values in a very limited low-lift range. From the low-lift-coefficient values of such

agreement to the highest values shown, the new method provides that less and less of the leading-edge force be manifested as thrust, and more and more be manifested as vortex lift. The inset flow-visualization photographs, taken at the conditions represented by the darkened symbols, are included to provide an understanding of the flow physics at those points. The upper pair of photographs are of the upper surfaces of the model with a fluorescent oil coating, which, under the action of the flow, has essentially stabilized at each of the two conditions. The picture at the right is taken from above the right rear quadrant of the model as it is immersed in humid, partially condensed flow and illuminated by a thin fan of intense light positioned normal to the flow. Strong vortices appear at this high-lift condition as the pair of dark circles located above the wing surface about midway between the wing leading edges and the model plane of symmetry. Thus the upper-surface flow appears to vary from the classic potential-flow condition at the lift coefficient for which the wing camber was designed, through a condition in which there is a mixed flow including some vorticity, to the condition at high lifts in which there is strong, fully separated vorticity located well inboard of the leading edge. In any event, the modified linear theory method, which attempts to account for these nonlinear types of flow, provides, in addition to an indication of significant amounts of leading-edge thrust, a substantially improved representation of the experimental results. Note for future reference that angles of attack of 2 and 4 degrees fall just below and above that for maximum lift-drag ratio.

Spanwise Distribution of Thrust

With supersonic thrust distribution being so critically dependent upon the degree to which the leading edge is swept behind the Mach line, consideration of the spanwise distribution of thrust in figure 7 begins with the spanwise distribution of a parameter, $1/(\beta \cot \Lambda)$, which is the ratio of the tangent of the leading-edge sweep to the tangent of the sweep of the Mach line. Thus, the higher the values of $1/(\beta \cot \Lambda)$, the more subsonic the leading edge, with the value of unity representing a sonic leading edge, and lesser values corresponding to a supersonic leading edge. The calculated values of local thrust coefficient for the experimental configuration at test Reynolds number (2.07×10^6) and at design Mach number (1.8) are shown divided by α^2. This is a convenient way to express local thrust, since theoretical maximum thrust coefficient is a direct function of α^2 and the aim here is to show that as angle of attack is increased the portion of maximum theoretical thrust which appears to be attainable becomes smaller. It should be recalled that the theory assumes that attainable thrust is that component of maximum theoretical thrust which manifests itself as thrust, while the normal component of that theoretical maximum manifests itself as vortex lift, with the difference between the $C_{t,max}$ and C_t curves defining the location and intensity of the latter. Thus, theoretically, the loss of thrust and the attendant development of vortex lift begins outboard and moves progressively inboard as angle of attack is increased. This analytical degradation in percent of maximum theoretical thrust and the corresponding increase in vortex lift, as angle of attack is increased from 2 to 4 degrees in this figure, correspond to the lift-drag-ratio decrements between full and attainable thrust at these two angles in

figure 6. The calculated values of both figures 6 and 7 indicate the effect of considerable vorticity at the higher angle (4°), with the former (figure 6) providing strong experimental evidence in the corresponding oil-flow photograph.

Lest it be assumed that attainable thrust decreases with increasing angle of attack, the remaining thrust-distribution figures, beginning with figure 8, will deal in absolute values of local thrust coefficient at the two angles of attack of 2 and 4 degrees. In fact, they will show that calculated attainable thrust at 4 degrees exceeds, in most cases, the theoretical maximum thrust at 2 degrees angle of attack.

The calculated values of absolute local thrust coefficients in figure 8 are for the same conditions as in the previous figure, except that values for a full-scale Reynolds number of 128 million (corresponding to $\bar{c}$ = 25.3 meters and an altitude of 17400 meters) have been added. For convenience, the value of total thrust coefficient C_T, which is twice the integral of the local coefficients, is shown for each Reynolds number. At an angle of attack of two degrees, thrust loss begins near midsemispan and there is a count (0.0001) or so difference in the total thrust coefficient between Reynolds numbers of 2.07 million and 128 million, with the value for 128 million being about two counts less than the theoretical maximum value (RN = ∞). At four degrees however, there is an appreciable difference in location of thrust loss and nearly five counts difference between tunnel and full-scale Reynolds number, with that for the latter being approximately half the 34-count theoretical maximum value. In this case, the effects of Reynolds number on thrust are seen to be important, but certainly not critical.

The local thrust coefficient values of figure 9 are for the same basic configuration at a Reynolds number of 128 million, but with another Mach number, 1.4, as well as the original 1.8. While the spanwise location of thrust loss here does not appear to be strongly Mach-number dependent, both the attainable and theoretical maximum values of total thrust appear to be very much so. At both angles of attack, attainable thrust at Mach number 1.4 is about double that at Mach number 1.8, with some 35-1/2 counts appearing to be attainable out of the 65 counts of theoretical maximum thrust at M = 1.4. The fact that, at both two and four degrees, the calculations show full thrust to extend somewhat further out on the wing semispan at Mach number 1.4 than at 1.8 is surprising, since the inboard leading edge contains a significant portion swept at 79-1/2 degrees--a very subsonic segment with a normal Mach number of 0.255. This suggests that design values of $1/(\beta \cot \Lambda)$ might be significantly increased over those of the present wing at Mach number 1.8.

In figure 10, calculated local thrust coefficients for a Mach number of 1.8 and a Reynolds number of 128 million are shown for the basic configuration with its 4-percent-thick wing, and for variations in wing thickness to 3 and 5 percent. Qualitatively, the inboard progression of thrust loss with decreasing thickness is as would be expected. As was the case for Reynolds-number variation in figure 8, the effect of the present variable (t/c) is seen, within the range shown (0.03 to 0.05), to be important to leading-ledge thrust, but certainly not critical.

Thrust-Dependent Lift-Drag Ratio

The previous thrust-distribution figures (8, 9, and 10) have shown, for the basic study configuration and variations thereof, the dependence of leading-edge thrust on Reynolds number, Mach number, and thickness ratio. Figure 11 addresses the effects of these same three variables (RN, M, and t/c) on maximum lift-drag ratio, including leading-edge thrust effects. In each case, the theoretical curves for full leading-edge thrust, no leading-edge thrust, and attainable thrust are shown. Where available, the appropriate experimental points are presented. Unless otherwise indicated on an abscissa, Mach number is 1.8 and thickness ratio is 0.04.

The large effect on maximum lift-drag ratio of the variation of Reynolds number is almost entirely that due to the change in viscous drag. Calculated attainable thrust is seen to vary from about half the increment between no thrust and full thrust at the lowest Reynolds number to about 60 percent at the highest--a small amount compared to that due to the viscous-drag change. The agreement between experiment and calculation seems reasonably good.

The effect on maximum lift-drag ratio of varying Mach number over the range shown is particularly large for the full-thrust case at both the test and full-scale Reynolds numbers, with the attainable-thrust curve showing a similarly large variation at the high Reynolds number. In contrast, the attainable-thrust variation at test Reynolds number (2.07 million) falls about midway between the full-thrust values and those for the relatively insensitive no-thrust curve. This greater thrust dependency on Mach number certainly suggests that the extrapolations of such wind-tunnel data to full-scale conditions take careful account of leading-edge thrust. Again, agreement between experiment and calculation is reasonably good, but particularly significant to the designer is that agreement at the $M = 1.5$ condition, for it suggests that very high values of $1/(\beta \cot \Lambda)$ (or very low Mach-number components normal to the wing leading edge) may be tolerated.

The sharp variations of maximum lift-drag ratio with thickness ratio is again seen to be an effect on mimimum drag. Here, it is a large variation of zero-lift wave drag with thickness. The steeper variation at the full-scale Reynolds number is due to the combining of the additional viscous-drag decrement with the sharply changing wave drag to produce, as thickness is reduced, very low values of minimum drag and consequently high lift-drag ratios. An interesting additional point is that, at full-scale Reynolds number, values of maximum lift-drag ratio corresponding to the attainable-thrust curve did not fall off toward the no-thrust curve as thickness decreased.

It is to be noted that supersonic-cruise designs have generally been based on analytical methods which excluded leading-edge thrust, corresponding to the dashed-curve values of figure 11. In the light of the experimentally and analytically indicated high tolerance to high values of $1/(\beta \cot \Lambda)$ (lower Mach numbers, here) and the calculatively indicated insensitivity of thrust to thickness (for moderate changes in thickness), very high levels of supersonic aerodynamic performance seem possible.

Returning via figure 12 to the spanwise variation of the design parameter, $1/(\beta \cot \Lambda)$, upon which leading-edge thrust is so dependent, an additional curve (beyond that shown in figure 7) corresponding to the basic configuration at a Mach number of 1.5 has been added as the dashed line. It is this much more subsonic leading edge which appears to have worked well at M = 1.5. The leading edge of a new wing with a design Mach number of 1.8, but with the same spanwise schedule of $1/(\beta \cot \Lambda)$ as the original wing (A) at Mach number 1.5, is defined by the indicated integration of the dashed curve. Requiring, in addition, the same tip chord, the same chord as at the trailing-edge break, and the same wing area as (A) results in the new wing (B) . Calculated maximum lift-drag ratio and the product of it and Mach number are shown for 4-percent-thick versions of both wings (A) and (B) at Mach numbers 1.5 and 1.8 and at test and full-scale Reynolds numbers in figure 13. The available corresponding experimental values are also shown as the circle symbols. An interesting result shown in this figure is that, at full-scale Reynolds number, both maximum L/D and M·L/D are higher for wing (B) at M = 1.8 than for wing (A) at either Mach number. From this point, a designer might profitably trade toward lower outboard panel sweep without significant performance loss and then trade toward a thickness substantially less than the present 4 percent so as to produce extraordinarily high levels of aerodynamic performance.

Additional Design Considerations

Taking a broader view of wings designed to operate at cruise with a significant amount of leading-edge thrust, several design-oriented observations can be made with the aid of figure 14. Here the planform of the present study is shown shaded and superimposed on the containing delta planform. Recognizing the seeming inevitable shrinkage in wing size (to reduce wetted area and weight) in the successive stages of design cycling from the initial concept, the lower half of the planform figure was prepared to show the containing delta and a shrunken version thereof having the same plan area as shaded above. Immediately apparent is its much-reduced effective lifting length and shorter span compared to the initial shaded planform. Considering that supersonic drag due to lift is an inverse function of the combination of the square of the lifting length and the square of the span, it is critically important to aerodynamic performance to be particularly selective in reducing wing area. The shaded planform reduces wing area but preserves the overall length and span, and thus should tend to retain the aerodynamic efficiency of the larger containing delta. Another point regarding the shaded planform is that structurally it should tend to resemble a wing having the planform represented by the shaded area rearward of the short-dash line, but to which has been added a forward strake.

A final point to be made through this figure is in regard to treatment of the planform at the wing tip. It is suggested that the wing tip be tailored to provide that the tip vortex initiate inboard along the leading edge so as to place not only its suction effect on the upper surface but its pumping or scavenging effect over the tip area which might otherwise experience flow separation as in the inset sketch below.

CONCLUDING REMARKS

There are several observations growing out of the present study which should be of interest to the designer of supersonic-cruise vehicles. Foremost is that experimental results indicate the presence of significant amounts of leading-edge thrust at supersonic speeds. Furthermore, there is a new methodology for the prediction of attainable leading-edge thrust and/or that component of thrust which acts as vortex lift. There is, as well, a new class of supersonic wings which matches the theoretical thrust-distribution potential with supporting airfoil geometry (that is, which places upwash where there is bluntness). These should lead to higher maximum lift-drag ratios at higher lift coefficients. Noting that with the attainment of substantial amounts of leading-edge thrust at supersonic speeds increasing with diminishing Mach numbers, efforts to significantly improve range factor ($M \cdot L/D \div sfc$) should give rise to serious consideration of lower supersonic-cruise speeds (of the order of Mach number 2 or less). These lower speeds will certainly offer more speed-compatible airframes and propulsion systems.

REFERENCES

1. Robins, A. Warner; Lamb, Milton; and Miller, David S.: Aerodynamic Characteristics at Mach Numbers of 1.5, 1.8, and 2.0 of a Blended Wing-Body Configuration With and Without Integral Canards. NASA TP-1427, 1979.

2. Robins, A. W.; and H. W. Carlson: High Performance Wings With Significant Leading-Edge Thrust at Supersonic Speeds. Presented at AIAA Aircraft Systems and Technology Meeting, August 20-22, 1979, New York, New York.

3. Morris, Odell A.; and Fournier, Roger H.: Aerodynamic Characteristics at Mach Numbers 2.30, 2.60, and 2.96 of a Supersonic Transport Model Having a Fixed, Warped Wing. NASA TM X-1115, 1965.

4. Harris, Roy V., Jr. An Analysis and Correlation of Aircraft Wave Drag. NASA TM X-947, 1964.

5. Middleton, Wilbur D.; and Carlson, Harry W.: Numerical Method of Estimating and Optimizing Supersonic Aerodynamic Characteristics of Arbitrary Planform Wings. J. Aircraft, vol. 2, no. 4, July-August, 1965, pp. 261-265.

6. Sommer, Simon C.; and Short, Barbara J.: Free-Flight Measurements of Turbulent-Boundary-Layer Skin Friction in the Presence of Severe Aerodynamic Heating at Mach Numbers From 2.8 to 7.0. NACA TN 3391, 1955.

7. Middleton, W. D.; and Lundry, J. L.: A Computational System for Aerodynamic Design and Analysis of Supersonic Aircraft. Part I - General Description and Theoretical Development. NASA CR-2715, 1976.

8. Middleton, W. D.; Lundry, J. L; and Coleman, R. G.: A Computational System for Aerodynamic Design and Analysis of Supersonic Aircraft. Part 2 - User's Manual. NASA CR-2716, 1976.

9. Middleton, W. D.; Lundry, J. L.; and Coleman, R. G.: A Computational System for Aerodynamic Design and Analysis of Supersonic Aircraft. Part 3 - Computer Program Description. NASA CR-2717, 1976.

10. Polhamus, Edward C.: Predictions of Vortex-Lift Characteristics by a Leading-Edge Suction Analogy. J. Aircraft, vol. 8, no. 4, April 1971, pp. 193-199.

11. Kulfan, R. M.: Wing Geometry Effects on Leading Edge Vortices. Presented at AIAA Aircraft Systems and Technology Meeting, August 20-22, 1979, New York, New York.

12. Carlson, Harry W.; and Mack, Robert J.: Estimation of Leading-Edge Thrust for Supersonic Wings of Arbitrary Planform. NASA TP-1270, 1978.

13. Carlson, Harry W.; Mack, Robert J.; and Barger, Raymond L.: Estimation of Attainable Leading-Edge Thrust for Wings at Subsonic and Supersonic Speeds. NASA TP-1500, 1979.

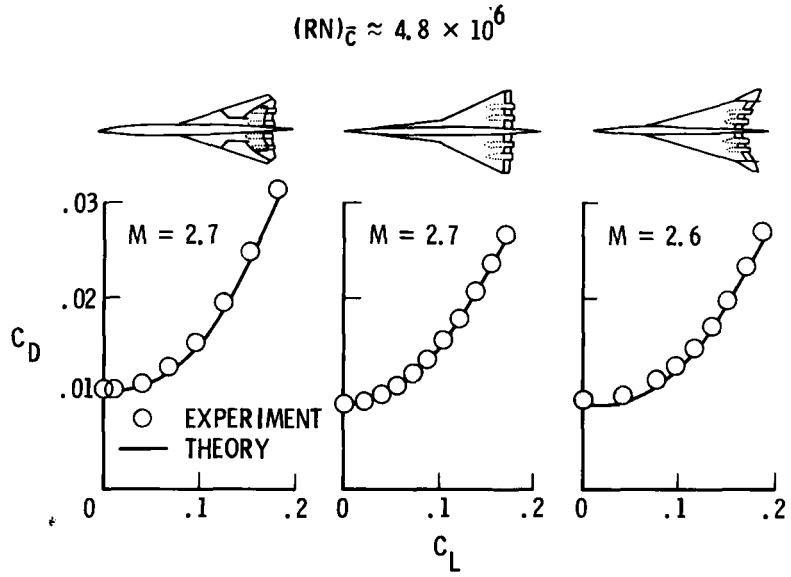

Figure 1.- Experimental/theoretical drag polars of models of supersonic-cruise aircraft.

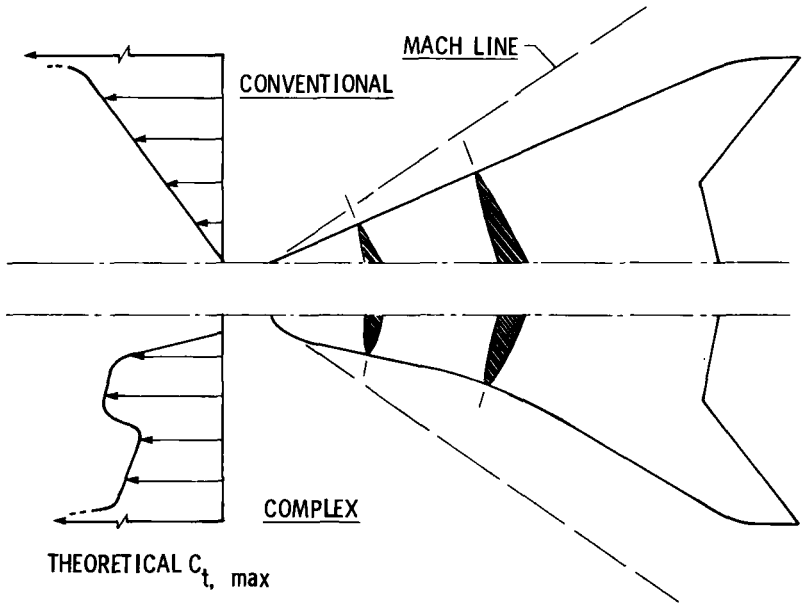

Figure 2.- Thurst and thickness comparisons near wing leading edge.

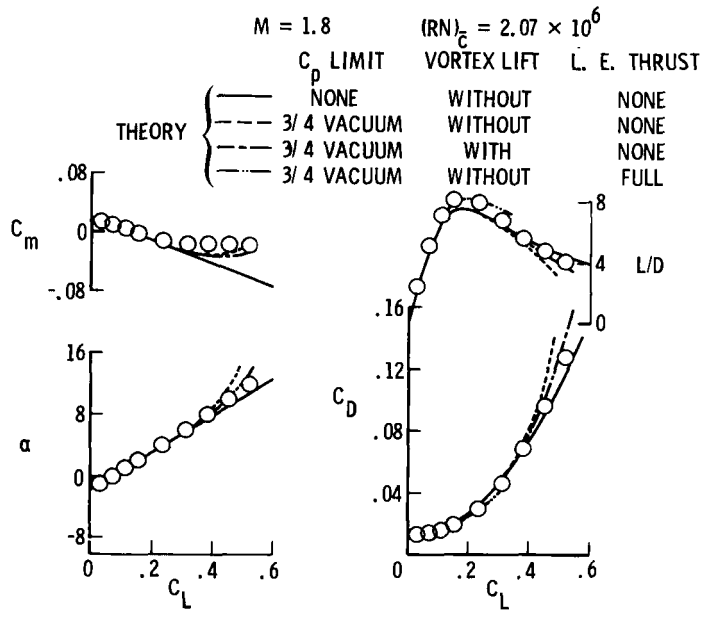

Figure 3.- Experimental/theoretical comparisons of longitudinal aerodynamic characteristics.

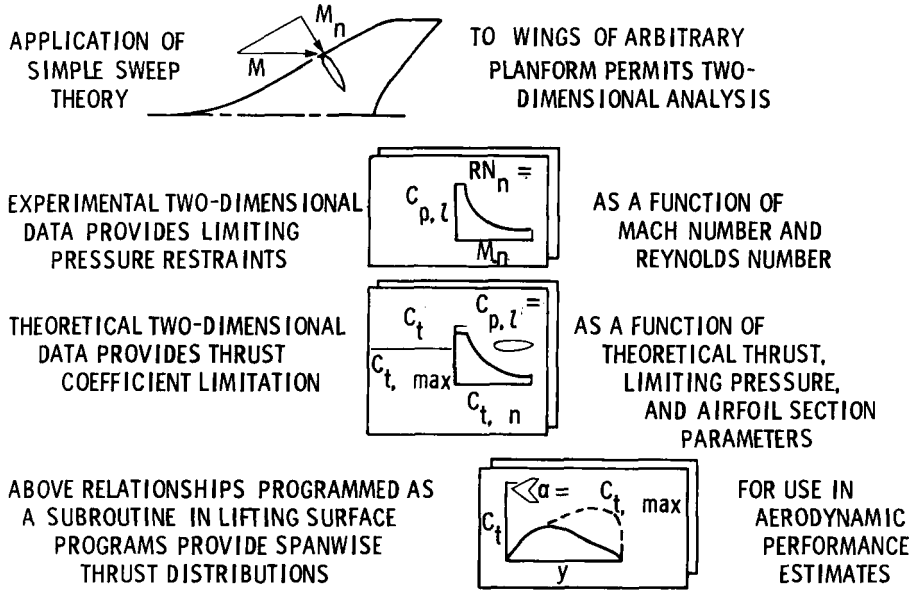

Figure 4.- Key features of attainable-thrust prediction method.

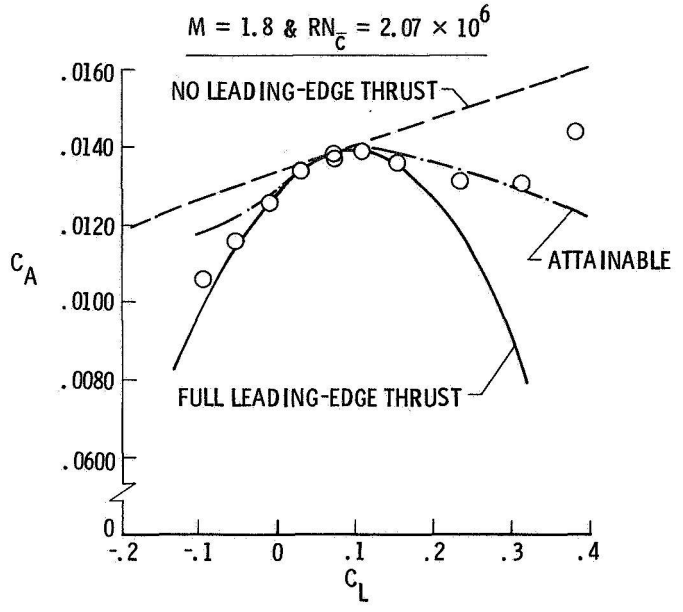

Figure 5.- Experimental/theoretical axial-force coefficients.

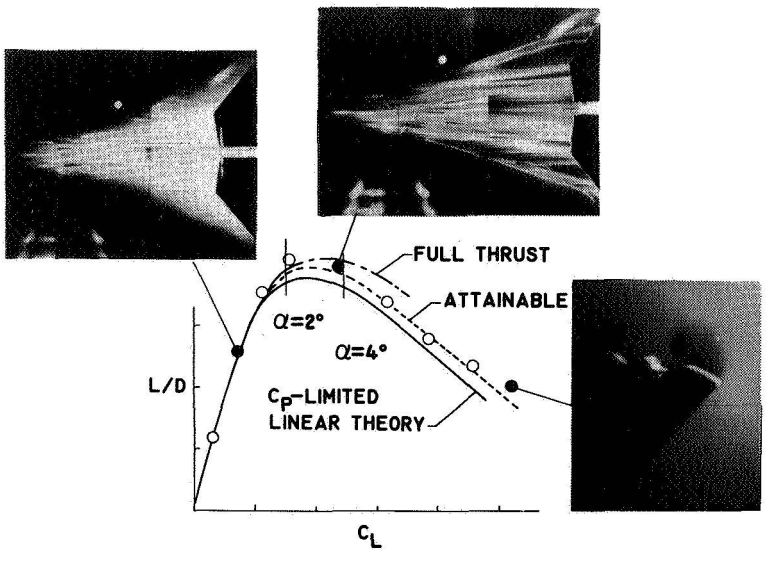

Figure 6.- Comparison of theories with both qualitative and quantitative experimental data.

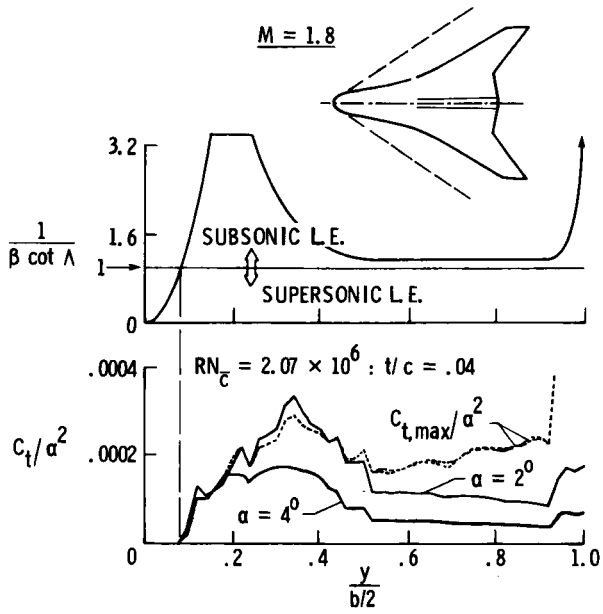

Figure 7.- Spanwise distribution of leading-edge thrust.

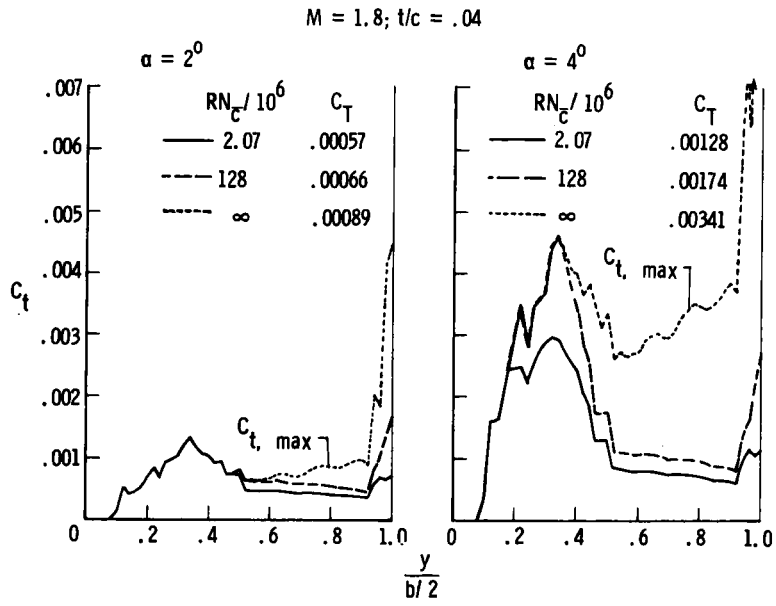

Figure 8.- L. E. thrust dependency on Reynolds number.

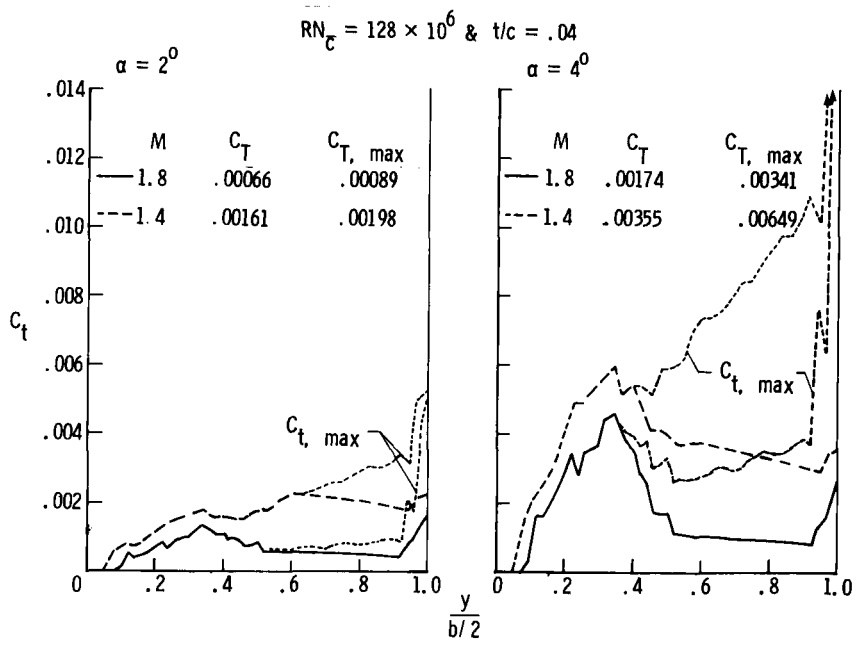

Figure 9.- L. E. thrust dependency on Mach number.

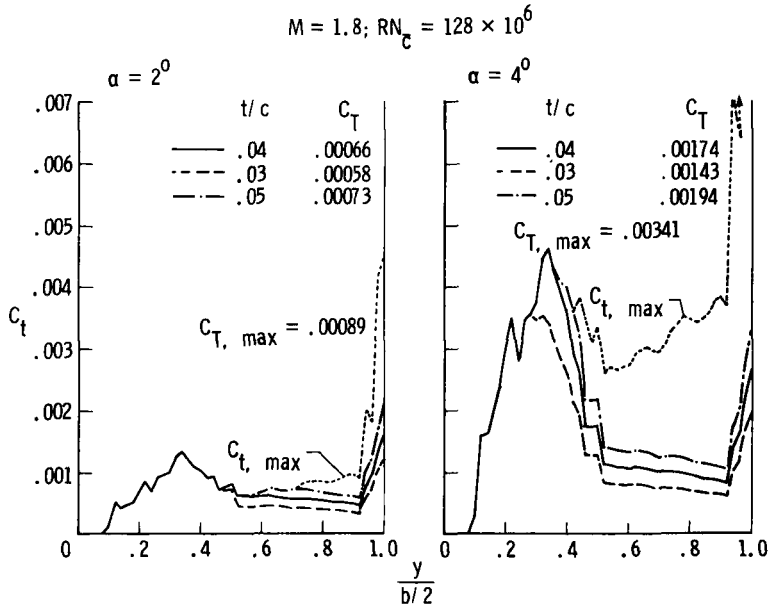

Figure 10.- L. E. thrust dependency on thickness ratio.

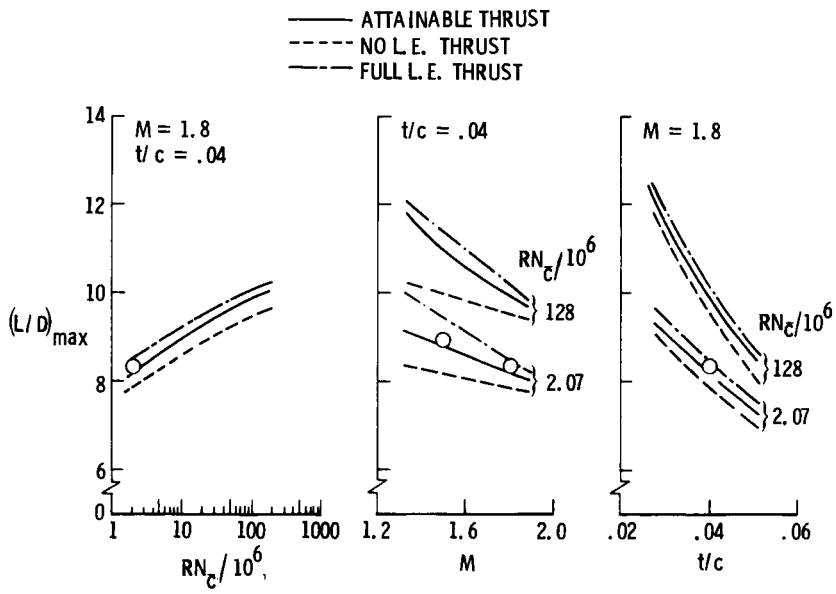

Figure 11.- Maximum lift/drag ratio as affected by Reynolds & Mach numbers & thickness.

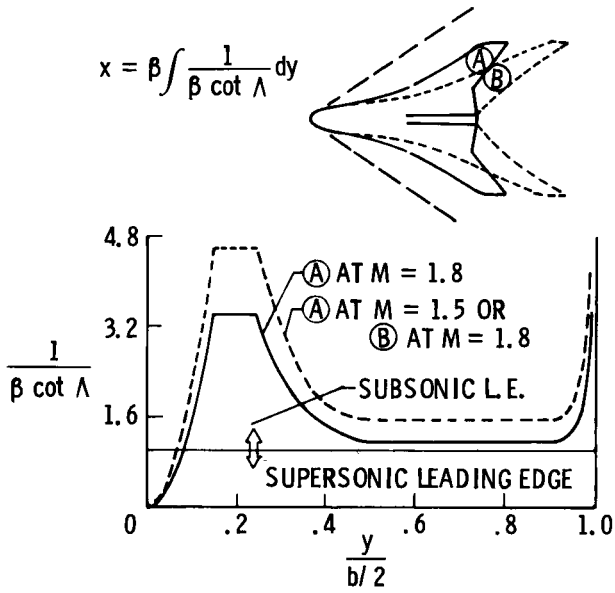

Figure 12.- Generation of alternate wing.

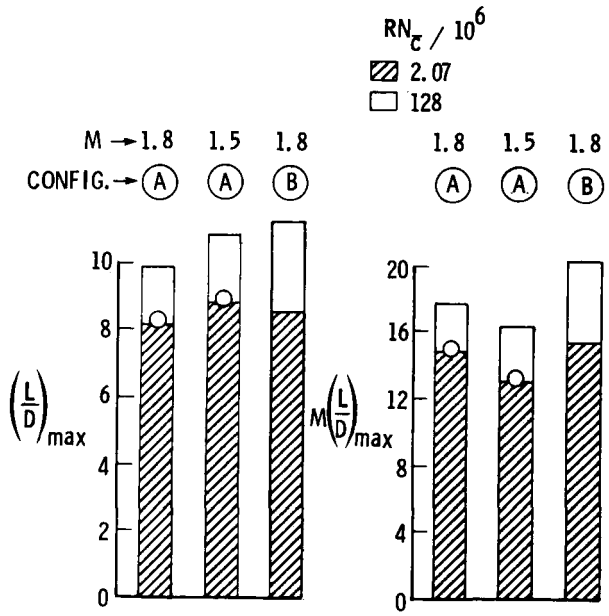

Figure 13.- Aerodynamic performance of original & alternate wings.

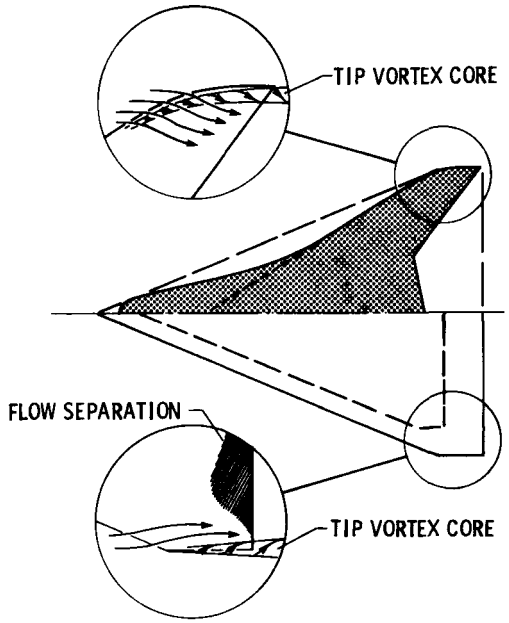

Figure 14.- Additional design considerations.